

Determination of the chemical potential in the Tsallis distribution at LHC energies.

J. Cleymans¹, M.W. Paradza^{1,2}

¹ *UCT-CERN Research Centre and Department of Physics,
University of Cape Town, Rondebosch 7701, Cape, Republic of South Africa*

² *Cape Peninsula University of Technology, Cape Town, South Africa.*

Abstract

The transverse momentum distributions measured in $p - p$ collisions at the LHC determine the kinetic freeze-out stage of the collision. The parameters deduced from these distributions differ from those determined at chemical freeze-out. The present investigation focuses on the chemical potentials at kinetic freeze-out, these are not necessarily zero as they are at chemical freeze-out, the only constraint is that they should be equal for particles and antiparticles at LHC energies. The thermodynamic variables are determined in the framework of the Tsallis distribution. The chemical potentials in the Tsallis distribution analysis of $p - p$ collisions at four different LHC energies have correctly been taken into account. This leads to a much more satisfactory analysis of the various parameters and confirms the usefulness of the Tsallis distribution in high-energy collisions. In particular we find that the temperature T and the volume V at each beam energy are the same for all particle types considered (pions, kaons and protons). The chemical potentials for these particles are however very different. Hence we conclude that there is evidence for thermal equilibrium at kinetic freeze-out, albeit in the sense of the Tsallis distribution and there is no evidence for chemical equilibrium at the final stage of the collision.

Keywords: Tsallis distribution, Transverse Momentum, Particle Production

1. Introduction

The Tsallis distribution [1] was first proposed more than three decades ago as a generalization of the Boltzmann-Gibbs distribution and is characterized

by an additional parameter q which measures the deviation from a standard Boltzmann-Gibbs distribution. Over the past few years it has also been applied to high-energy physics where it has been successful in describing the transverse momentum distributions in $p - p$ collisions [2, 3, 4, 5, 6, 7, 8, 9, 10, 11, 12, 13, 14, 15, 16, 17, 18, 19] (for a recent review see e.g. [20]).

One particular form, which satisfies thermodynamic consistency relations [21, 22] is given by:

$$E \frac{d^3 N}{d^3 p} = g V E \frac{1}{(2\pi)^3} \left[1 + (q-1) \frac{E - \mu}{T} \right]^{-\frac{q}{q-1}}, \quad (1)$$

where V is the volume, q is the Tsallis parameter and T is the corresponding temperature or, in terms of variables commonly used in high-energy physics, rapidity y , transverse mass $m_T = \sqrt{p_T^2 + m^2}$:

$$\frac{d^2 N}{dp_T dy} = g V \frac{p_T m_T}{(2\pi)^2} \left[1 + (q-1) \frac{m_T \cosh y - \mu}{T} \right]^{-\frac{q}{q-1}}. \quad (2)$$

In the limit where the parameter q tends to unity one recovers the well-known Boltzmann-Gibbs distribution:

$$\lim_{q \rightarrow 1} \frac{d^2 N}{dp_T dy} = g V \frac{p_T m_T}{(2\pi)^2} \exp \left(-\frac{m_T \cosh y - \mu}{T} \right). \quad (3)$$

The main advantage of Eq. (2) over Eq. (3) is that it has a polynomial decrease with increasing p_T which is what is observed experimentally.

It was recognized early on [13] that there is a redundancy in the number of parameters in this distribution, namely the four parameters T, V, q, μ in Eq. (2) can be replaced by just three parameters T_0, V_0, q with the help of the following transformation:

$$T_0 = T \left[1 - (q-1) \frac{\mu}{T} \right], \quad \mu \leq \frac{T}{q-1}, \quad (4)$$

$$V_0 = V \left[1 - (q-1) \frac{\mu}{T} \right]^{\frac{q}{1-q}}, \quad (5)$$

leading to a transverse momentum distribution which can thus be written equivalently as

$$\frac{d^2 N}{dp_T dy} = g V_0 \frac{p_T m_T}{(2\pi)^2} \left[1 + (q-1) \frac{m_T \cosh y}{T_0} \right]^{-\frac{q}{q-1}}. \quad (6)$$

where the chemical potential does not appear explicitly.

It thus requires special attention to determine the chemical potential using the above Tsallis distribution when fitting experimental data.

It is to be noted that most previous analyses have confused the two equations (2) and (6) and reached conclusions that are incorrect, namely that at LHC energies, different hadrons, π, K, p, \dots cannot be described by the same values of T and V . As we will show this is based on using T_0 and V_0 and not T and V . Many authors have followed this conclusion because at LHC energies equal numbers of particles and antiparticles are being produced and, furthermore, at chemical equilibrium, one has indeed $\mu = 0$ for all quantum numbers. However the equality of particle and antiparticle yields, at thermal freeze-out, only implies that e.g. π^+ and π^- have the same chemical potential but they are not necessarily zero.

It is the purpose of the present paper to resolve this issue. The procedure we choose is the following:

1. Use Eq. (6) to fit the transverse momentum distributions. This determines the three parameters T_0, q and V_0 .
2. Fix the parameter q thus obtained.
3. Perform a new fit to the transverse momentum distributions using Eq. (1) keeping q as determined in the previous step. This determines the parameters T and V and the chemical potential μ .
4. Check the consistency with Eqs. (4) and (5).

Each step in the fitting procedure thus involves only three parameters to describe the transverse momentum distributions.

We emphasize that the chemical potentials at kinetic freeze-out (described here with a Tsallis distribution), are not related to those at chemical freeze-out. At chemical freeze-out, where thermal and chemical equilibrium have been well established the chemical potentials are zero. At kinetic freeze-out however, there is no chemical equilibrium and the observed particle-antiparticle symmetry only implies that the chemical potentials for particles must be equal to those for antiparticles. However, due to the absence of chemical equilibrium they do not have to be zero. The only constraint is that they should be equal for particles and antiparticles.

As mentioned above, the advantage of using the above distribution is that they follow consistent set of thermodynamic relations

$$d\epsilon = T ds + \mu dn, \tag{7}$$

$$dP = s dT + n d\mu, \quad (8)$$

namely, with the distribution

$$f(E, q, T, \mu) \equiv \left[1 + (q - 1) \frac{E - \mu}{T} \right]^{-\frac{1}{q-1}}, \quad (9)$$

and

$$n \equiv g \int \frac{d^3p}{(2\pi)^3} f^q, \quad (10)$$

$$\epsilon \equiv g \int \frac{d^3p}{(2\pi)^3} E f^q, \quad (11)$$

$$s = -g \int \frac{d^3p}{(2\pi)^3} [f^q \ln_q f - f], \quad (12)$$

$$P \equiv g \int \frac{d^3p}{(2\pi)^3} \frac{p^2}{3 E} f^q. \quad (13)$$

where ϵ is the energy density, T is the temperature, s is the entropy density, P is the pressure, μ is the chemical potential and n is the particle density. It was shown (see [21, 22, 23] for more details) that n, ϵ, s and P given by the following relations:

It is thus clear that the parameter T can now now considered as a temperature in the thermodynamic sense:

$$T = \left. \frac{\partial E}{\partial S} \right|_{V, N}, \quad (14)$$

where the entropy S is the Tsallis entropy.

It is the purpose of the present paper to determine the chemical potential using the above Tsallis distribution when fitting experimental data.

2. Fits without chemical potentials using Eq. (6).

The Tsallis distribution has been widely used in the analysis of transverse momentum spectra [2, 3, 4, 5, 6, 7, 8, 9, 10, 11, 12, 13, 14, 15, 16, 17, 18, 19]. Most of these put the chemical potential equal to zero and therefore use Eq. (6). We can therefore take over their results which we reinterpret as being for T_0, V_0 and q . The results obtained are reproduced in Table 1.

No new fits are made and we base our results on those reported in a recent analysis [24]. It is to be noted that e.g. in $p-p$ collisions at $\sqrt{s} = 7$ TeV the radius varies between 3 and 5.7 fm while the temperature T_0 varies between 66 and 101 MeV.

3. Tsallis Fits with Chemical Potential Using Eq. (2)

\sqrt{s} (TeV)	Particle	R_0 (fm)	q	T_0 (GeV)	χ^2 / NDF
0.9 [25]	π^+	4.835 ± 0.136	1.148 ± 0.005	0.070 ± 0.002	22.73 / 30
	π^-	4.741 ± 0.131	1.145 ± 0.005	0.072 ± 0.002	15.83 / 30
	K^+	4.523 ± 1.302	1.175 ± 0.017	0.057 ± 0.013	13.02 / 24
	K^-	3.957 ± 0.962	1.161 ± 0.016	0.064 ± 0.013	6.214 / 24
	p	42.72 ± 19.8	1.158 ± 0.006	0.020 ± 0.004	14.29 / 21
	\bar{p}	7.445 ± 3.945	1.132 ± 0.014	0.052 ± 0.016	13.82 / 21
2.76 [26]	$\pi^+ + \pi^-$	4.804 ± 0.100	1.149 ± 0.002	0.077 ± 0.001	20.64 / 60
	$K^+ + K^-$	2.51 ± 0.128	1.144 ± 0.002	0.096 ± 0.004	2.459 / 55
	$p + \bar{p}$	4.009 ± 0.623	1.121 ± 0.005	0.086 ± 0.008	3.509 / 46
5.02 [27]	$\pi^+ + \pi^-$	5.025 ± 0.111	1.155 ± 0.002	0.076 ± 0.002	20.13 / 55
	$K^+ + K^-$	2.437 ± 0.168	1.15 ± 0.005	0.099 ± 0.006	1.516 / 48
	$p + \bar{p}$	3.601 ± 0.546	1.126 ± 0.005	0.091 ± 0.009	2.558 / 46
7.0 [27, 28]	$\pi^+ + \pi^-$	5.664 ± 0.167	1.179 ± 0.003	0.066 ± 0.002	14.14 / 38
	$K^+ + K^-$	2.511 ± 0.145	1.158 ± 0.005	0.097 ± 0.005	3.114 / 45
	$p + \bar{p}$	3.074 ± 0.405	1.124 ± 0.005	0.101 ± 0.008	6.031 / 43

Table 1: Fit results at $\sqrt{s} = 900$ GeV [25], $\sqrt{s} = 2.76$ TeV [26], 5.02 TeV [27] and 7 TeV [27, 28], using data from the ALICE collaboration, with μ fixed to zero using Eq. (6).

The fits to the transverse momentum distributions were then repeated using Eq. (2) but this time keeping the parameter q fixed to the value determined in the previous section and listed in Table 1. The results are listed in Table 2, where we present the fit results for non-zero chemical potential for $p-p$ collisions at four different beam energies by the ALICE collaboration.

It is to be noted that the entry for the proton at 900 GeV has a very large uncertainty; for this reason we also considered the results obtained by the CMS collaboration [29] at the LHC. The results are shown in Tables 3 and 4, in this case the proton can be determined more accurately.

\sqrt{s} (TeV)	Particle	R (fm)	μ (GeV)	T (GeV)	χ^2 / NDF
0.9 [25]	π^+	4.228 ± 0.276	0.159 ± 0.014	0.094 ± 0.002	23.018 / 30
	π^-	4.34 ± 0.256	0.151 ± 0.015	0.094 ± 0.002	15.776 / 30
	K^+	4.313 ± 10.5	0.112 ± 0.476	0.077 ± 0.077	13.019 / 23
	K^-	4.367 ± 0.362	0.095 ± 0.027	0.080 ± 0.004	6.214 / 23
	p	3.922 ± 4.3	0.314 ± 0.216	0.067 ± 0.030	14.519/20
	\bar{p}	3.903 ± 0.296	0.218 ± 0.032	0.081 ± 0.003	13.830 / 20
2.76 [26]	$\pi^+ + \pi^-$	4.216 ± 2.521	-0.088 ± 0.100	0.064 ± 0.015	20.48/60
	$K^+ + K^-$	4.415 ± 3.783	-0.203 ± 0.130	0.058 ± 0.019	7.62 / 55
	$p + \bar{p}$	4.051 ± 5.033	-0.126 ± 0.234	0.070 ± 0.028	3.518/46
5.02 [27]	$\pi^+ + \pi^-$	4.394 ± 2.756	0.027 ± 0.130	0.080 ± 0.020	20.14 / 55
	$K^+ + K^-$	4.617 ± 5.828	-0.148 ± 0.255	0.078 ± 0.038	1.522 / 48
	$p + \bar{p}$	4.415 ± 5.191	-0.046 ± 0.267	0.085 ± 0.033	2.561/46
7.0 [27, 28]	$\pi^+ + \pi^-$	4.178 ± 0.287	0.192 ± 0.018	0.100 ± 0.003	14.15/38
	$K^+ + K^-$	4.205 ± 0.017	0.023 ± 0.005	0.102 ± 0.001	3.128 / 55
	$p + \bar{p}$	4.43 ± 0.298	0.070 ± 0.022	0.110 ± 0.003	6.031/43

Table 2: Fit results at $\sqrt{s} = 900$ GeV [25], $\sqrt{s} = 2.76$ TeV [26], 5.02 TeV [27] and 7 TeV [27, 28], using data from the ALICE collaboration with q from Table 1 following Eq. (2).

The conclusions remain unchanged: the results including the chemical potential lead to more consistent values for the temperature T and the radius R .

Focusing again on $p-p$ collisions at $\sqrt{s} = 7$ TeV the radius varies between 3 and 5.7 fm, the radius now varies between 4.18 and 4.4 fm instead of between 3 and 5.7 fm. The radii are now consistent with each other within error bars. The temperature T now varies between 100 and 110 MeV while previously the variation was between between 66 and 101 MeV. In general all values obtained are much more consistent with each other. This completely changes the overall picture obtained for the parameters obtained using the Tsallis distribution. The results for the temperature T are shown in Fig. 1. The uncertainties obtained at beam energies of 2.76 TeV and 5.02 TeV are large, it is to be hoped that these will be reduced in future analyses of the data. The results for the radii are shown in Fig. 2 where a similar picture emerges, namely radii at each beam energy are very similar for all the particle types considered. This lends support to the picture that the final state at kinetic freeze-out is in thermal equilibrium albeit in the Tsallis sense

\sqrt{s} (TeV)	Particle	R_0 (fm)	q	T_0 (GeV)	χ^2 / NDF
0.9 [29]	π^+	4.312 ± 0.123	1.164 ± 0.005	0.077 ± 0.002	4.044 / 19
	π^-	5.449 ± 0.158	1.167 ± 0.005	0.066 ± 0.002	10.3 / 19
	K^+	3.297 ± 0.984	1.158 ± 0.036	0.078 ± 0.022	2.123 / 14
	K^-	4.053 ± 1.918	1.182 ± 0.046	0.064 ± 0.027	1.236 / 14
	p	6.118 ± 3.725	1.139 ± 0.020	0.058 ± 0.022	9.596 / 24
	\bar{p}	8.619 ± 0.211	1.147 ± 0.001	0.047 ± 0.007	21.3 / 24
2.76 [29]	π^+	6.195 ± 0.201	1.189 ± 0.005	0.061 ± 0.002	5.711 / 19
	π^-	5.971 ± 0.186	1.184 ± 0.005	0.063 ± 0.002	7.077 / 19
	K^+	2.997 ± 0.826	1.162 ± 0.040	0.087 ± 0.024	2.447 / 14
	K^-	2.683 ± 0.685	1.147 ± 0.041	0.096 ± 0.024	7.407 / 14
	p	7.192 ± 0.170	1.166 ± 0.002	0.049 ± 0.001	27.43 / 24
	\bar{p}	3.028 ± 1.167	1.129 ± 0.025	0.087 ± 0.025	28.41 / 24
7.0 [29]	π^+	6.762 ± 0.246	1.203 ± 0.006	0.059 ± 0.002	14.29 / 19
	π^-	6.614 ± 0.233	1.202 ± 0.006	0.060 ± 0.002	11.36 / 19
	K^+	2.642 ± 0.588	1.152 ± 0.041	0.102 ± 0.024	2.074 / 14
	K^-	3.221 ± 1.422	1.186 ± 0.063	0.083 ± 0.036	4.38 / 14
	p	6.076 ± 0.145	1.184 ± 0.002	0.052 ± 0.001	12.22 / 24
	\bar{p}	7.394 ± 0.178	1.190 ± 0.002	0.045 ± 0.001	15.47 / 24
13.0 [30]	π^+	6.719 ± 0.305	1.215 ± 0.008	0.057 ± 0.003	3.546 / 19
	π^-	5.785 ± 0.222	1.191 ± 0.008	0.067 ± 0.003	12.72 / 19
	K^+	2.477 ± 0.071	1.142 ± 0.071	0.106 ± 0.041	1.828 / 14
	K^-	2.566 ± 1.667	1.155 ± 0.114	0.100 ± 0.065	1.323 / 14
	p	17.34 ± 7.603	1.206 ± 0.007	0.025 ± 0.007	8.921 / 24
	\bar{p}	6.516 ± 0.239	1.189 ± 0.003	0.048 ± 0.001	8.383 / 24

Table 3: Fit results using Eq. (6) at $\sqrt{s} = 900$ GeV, $\sqrt{s} = 2.76$ TeV, 5.02 TeV and 7 TeV, using data from the CMS collaboration.

of equilibrium.

Finally we show the chemical potentials at kinetic freeze-out as listed in Table 2 also in Fig. 3. We find that the chemical potentials are not always compatible with zero and can even be quite large. For example, for $p - p$ collisions at 7 TeV the chemical potential for pions is around 200 MeV while for kaons it is close to 20 MeV and for protons it is around 70 MeV. They are thus quite large, clearly non-zero and also very different from each other. This does not come as a surprise as no chemical equilibrium is expected to

\sqrt{s} (TeV)	Particle	R (fm)	μ (GeV)	T (GeV)	χ^2 / NDF
0.9 [29]	π^+	4.007 ± 0.104	0.137 ± 0.006	0.089 ± 0.001	4.056 / 19
	π^-	4.005 ± 0.014	0.191 ± 0.002	0.099 ± 0.001	10.74 / 19
	K^+	4.033 ± 0.138	0.089 ± 0.010	0.092 ± 0.001	2.123 / 14
	K^-	4.392 ± 0.015	0.097 ± 0.009	0.081 ± 0.001	1.236 / 14
	p	4.184 ± 0.126	0.184 ± 0.009	0.084 ± 0.001	9.596 / 24
	\bar{p}	4.112 ± 0.124	0.219 ± 0.009	0.079 ± 0.001	21.3 / 24
2.76 [29]	π^+	3.999 ± 0.103	0.211 ± 0.007	0.101 ± 0.001	5.712 / 19
	π^-	4.003 ± 0.102	0.208 ± 0.007	0.102 ± 0.001	7.077 / 19
	K^+	3.98 ± 0.136	0.079 ± 0.011	0.100 ± 0.001	2.447 / 14
	K^-	4.048 ± 0.014	0.053 ± 0.011	0.104 ± 0.002	7.407 / 14
	p	4.251 ± 0.025	0.186 ± 0.008	0.080 ± 0.001	27.43 / 24
	\bar{p}	4.198 ± 0.124	0.073 ± 0.011	0.099 ± 0.001	28.41 / 24
7.0 [29]	π^+	4.032 ± 0.104	0.204 ± 0.008	0.118 ± 0.001	235.7 / 19
	π^-	4.020 ± 0.102	0.202 ± 0.008	0.119 ± 0.001	240.4 / 19
	K^+	4.144 ± 0.144	0.045 ± 0.012	0.109 ± 0.002	2.074 / 14
	K^-	3.987 ± 0.140	0.092 ± 0.011	0.100 ± 0.002	4.38 / 14
	p	4.324 ± 0.025	0.160 ± 0.009	0.081 ± 0.001	12.22 / 24
	\bar{p}	4.418 ± 0.125	0.171 ± 0.009	0.078 ± 0.001	15.47 / 24
13.0 [30]	π^+	3.948 ± 0.154	0.207 ± 0.012	0.116 ± 0.001	138 / 19
	π^-	4.023 ± 0.015	0.211 ± 0.002	0.107 ± 0.001	12.72 / 19
	K^+	3.990 ± 0.264	0.039 ± 0.023	0.111 ± 0.003	1.828 / 14
	K^-	3.997 ± 0.267	0.045 ± 0.022	0.107 ± 0.004	1.323 / 14
	p	4.479 ± 0.194	-0.062 ± 0.020	0.112 ± 0.002	15.95 / 24
	\bar{p}	4.410 ± 0.189	0.155 ± 0.015	0.078 ± 0.001	80383 / 24

Table 4: Fit results using Eq. (2) at $\sqrt{s} = 900$ GeV, $\sqrt{s} = 2.76$ TeV, 5.02 TeV and 7 TeV, using data from the CMS collaboration with q from Table 3.

exist at kinetic freeze-out in $p-p$ collisions. We find the near equality of the values for T and R very interesting.

We have also checked the consistency of our results by comparing explicitly the values obtained for T_0 obtained by making use of Eq. (6) to those obtained by fitting the transverse momentum spectra using Eq. (2) combined with Eq. (4). The results are indeed consistent with each other within the errors of the analysis. This further confirms an assertion by [13] that there is a redundancy in the parameters appearing in Eq. (2).

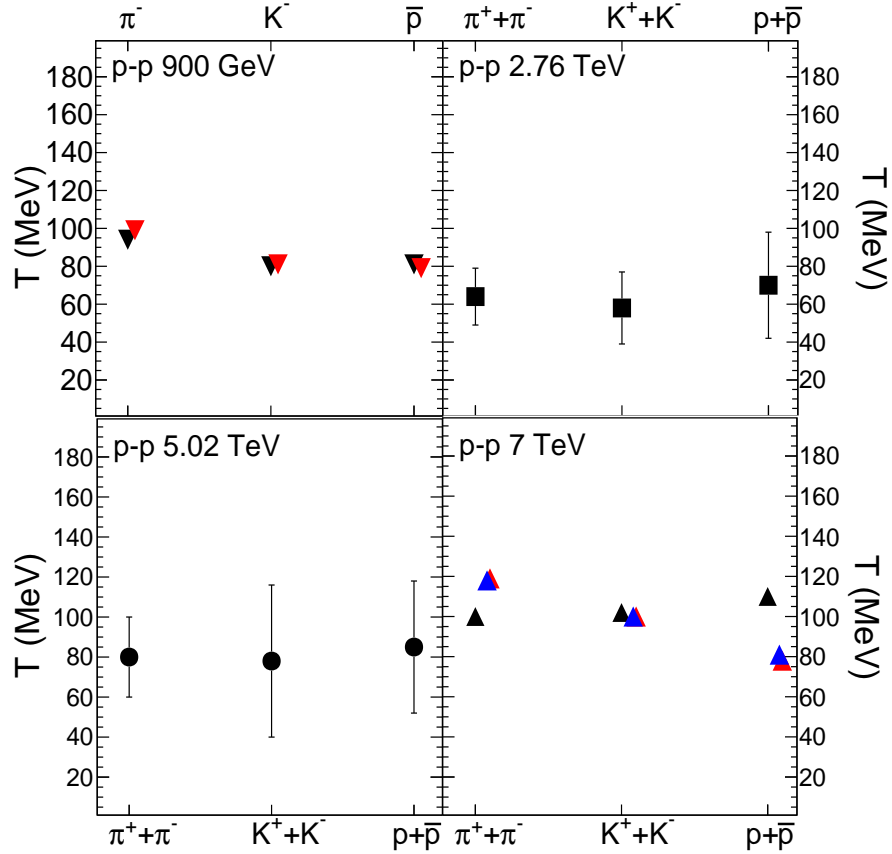


Figure 1: Values of T obtained by fitting data in $p-p$ collisions using Eq. (2). The upper-left plot was obtained using data at 900 GeV where the black triangles were obtained using data from the ALICE collaboration [25] while the red triangles use data from the CMS collaboration [29]. The upper-right plot uses data at 2.76 TeV [26], the lower-right plot is for 5.02 TeV [27] while the bottom-right plot is from $p-p$ data at 7 TeV [28]. In the last case we also show the results obtained from the CMS data [29], red is for negative hadrons, blue for positive ones.

4. Summary

A comparison of T and T_0 values for all the energies considered, for both the ALICE and CMS Collaborations are in agreement. This result confirms that the variables T, V, q , and μ in the Tsallis distribution function Eq. (1) have a redundancy for $\mu \neq 0$ [13].

The conclusions are as follows:

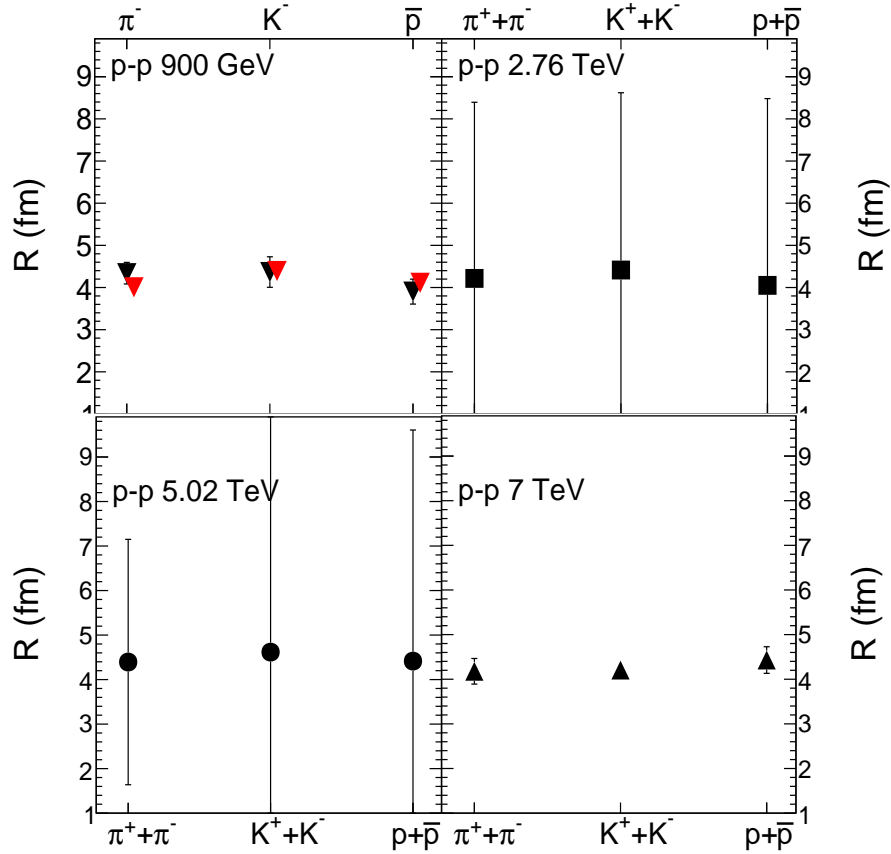


Figure 2: Radius as a function of particle type for four different beam energies in $p - p$ collisions obtained using Eq. (2) at mid-rapidity. The upper-left plot was obtained using data at 900 GeV where the black triangles were obtained using data from the ALICE collaboration [25] while the red triangles use data from the CMS collaboration [29]. the upper-right plot uses data at 2.76 TeV [26], the lower-right plot is for 5.02 TeV [27] while the bottom-right plot is from $p - p$ data at 7 TeV [28].

- The Tsallis distribution gives a good description of the transverse momentum spectra in $p - p$ collisions. These correspond to the thermal freeze-out stage in the collisions at LHC energies.
- There is a reasonable amount of thermal equilibrium even at the thermal freeze-out stage, albeit in the Tsallis thermodynamics sense. The resulting temperatures T are the same for all particle types considered.

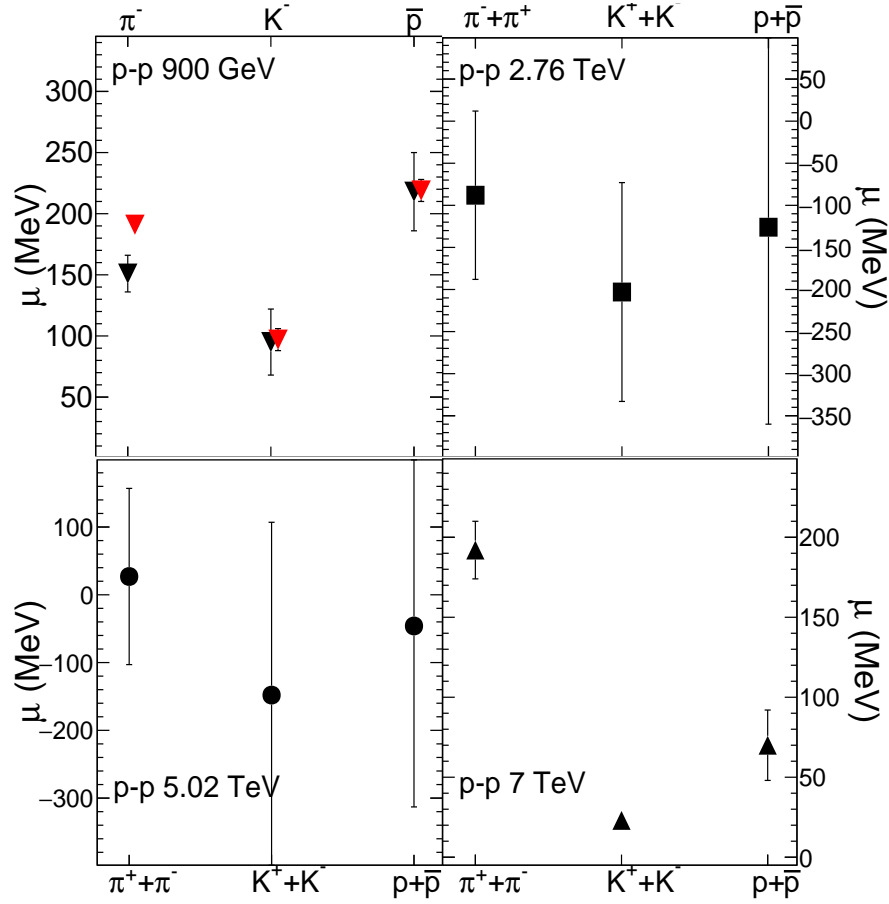


Figure 3: Chemical potential as a function of particle type. The upper-left plot was obtained using data at 900 GeV where the black triangles were obtained using data from the ALICE collaboration [25] while the red triangles use data from the CMS collaboration [29]. the upper-right plot uses data at 2.76 TeV [26], the lower-right plot is for 5.02 TeV [27] while the bottom-right plot is from $p - p$ data at 7 TeV [28].

This is in contrast to the results obtained in [24], the difference can be traced back to the incorrect use of chemical potentials in the latter analysis.

- The values obtained for the volume (or the radius shown in Fig. 2) are consistent with being equal for all particle types considered here. Admittedly the error bars are large at beam energies of 2.76 and 5.02 TeV for $p - p$ collisions.

- There is no chemical equilibrium at thermal freeze-out; the values obtained for μ for different particle types vary considerably.

In summary, in this work we have correctly taken into account the chemical potential in the Tsallis distribution analysis of $p-p$ collisions at four different LHC energies, this is summarized in the distinction that has to be made between T_0 as defined in Eq. (6) and T as defined in the starting Eq. (2). This leads to a much more satisfactory analysis of the various parameters and confirms the usefulness of the Tsallis distribution in high-energy collisions.

References

References

- [1] C. Tsallis, Possible Generalization of Boltzmann-Gibbs Statistics, *J. Statist. Phys.* 52 (1988) 479–487. doi:10.1007/BF01016429.
- [2] V. Cirigliano, G. M. Fuller, A. Vlasenko, A New Spin on Neutrino Quantum Kinetics, *Phys. Lett. B* 747 (2015) 27–35. arXiv:1406.5558, doi:10.1016/j.physletb.2015.04.066.
- [3] S. Grigoryan, Using the Tsallis distribution for hadron spectra in pp collisions: Pions and quarkonia at $\sqrt{s} = 5-13000$ GeV, *Phys. Rev. D* 95 (5) (2017) 056021. arXiv:1702.04110, doi:10.1103/PhysRevD.95.056021.
- [4] C.-Y. Wong, G. Wilk, L. J. Cirto, C. Tsallis, From QCD-based hard-scattering to nonextensive statistical mechanical descriptions of transverse momentum spectra in high-energy pp and $p\bar{p}$ collisions, *Phys. Rev. D* 91 (11) (2015) 114027. arXiv:1505.02022, doi:10.1103/PhysRevD.91.114027.
- [5] O. Ristea, C. Ristea, A. Jipa, Rapidity dependence of charged pion production at relativistic energies using Tsallis statistics, *Eur. Phys. J. A* 53 (5) (2017) 91. doi:10.1140/epja/i2017-12286-5.
- [6] G. Bíró, G. G. Barnaföldi, T. S. Biró, K. Ürmösy, Á. Takács, Systematic Analysis of the Non-extensive Statistical Approach in High Energy Particle Collisions - Experiment vs. Theory, *Entropy* 19 (2017) 88. arXiv:1702.02842, doi:10.3390/e19030088.

- [7] A. S. Parvan, Ultrarelativistic transverse momentum distribution of the Tsallis statistics, *Eur. Phys. J. A*53 (2017) 53. [arXiv:1607.07670](#), [doi:10.1140/epja/i2017-12242-5](#).
- [8] A. S. Parvan, O. V. Teryaev, J. Cleymans, Systematic Comparison of Tsallis Statistics for Charged Pions Produced In pp Collisions, *Eur. Phys. J. A*53 (5) (2017) 102. [arXiv:1607.01956](#), [doi:10.1140/epja/i2017-12301-y](#).
- [9] S. Tripathy, T. Bhattacharyya, P. Garg, P. Kumar, R. Sahoo, J. Cleymans, Nuclear Modification Factor Using Tsallis Non-extensive Statistics, *Eur. Phys. J. A*52 (9) (2016) 289. [arXiv:1606.06898](#), [doi:10.1140/epja/i2016-16289-4](#).
- [10] H. Zheng, L. Zhu, Comparing the Tsallis Distribution with and without Thermodynamical Description in $p + p$ Collisions, *Adv. High Energy Phys.* 2016 (2016) 9632126. [arXiv:1512.03555](#), [doi:10.1155/2016/9632126](#).
- [11] L. Marques, J. Cleymans, A. Deppman, Description of High-Energy pp Collisions Using Tsallis Thermodynamics: Transverse Momentum and Rapidity Distributions, *Phys. Rev. D*91 (2015) 054025. [arXiv:1501.00953](#), [doi:10.1103/PhysRevD.91.054025](#).
- [12] M. D. Azmi, J. Cleymans, The Tsallis Distribution at Large Transverse Momenta, *Eur. Phys. J. C*75 (9) (2015) 430. [arXiv:1501.07127](#), [doi:10.1140/epjc/s10052-015-3629-9](#).
- [13] J. Cleymans, G. I. Lykasov, A. S. Parvan, A. S. Sorin, O. V. Teryaev, D. Worku, Systematic properties of the Tsallis Distribution: Energy Dependence of Parameters in High-Energy p-p Collisions, *Phys. Lett. B*723 (2013) 351–354. [arXiv:1302.1970](#), [doi:10.1016/j.physletb.2013.05.029](#).
- [14] I. Sena, A. Deppman, Systematic analysis of p_T -distributions in $p + p$ collisions, *Eur. Phys. J. A*49 (2013) 17. [arXiv:1209.2367](#), [doi:10.1140/epja/i2013-13017-8](#).
- [15] M. D. Azmi, J. Cleymans, Transverse momentum distributions in proton–proton collisions at LHC energies and Tsallis thermodynam-

- ics, *J. Phys. G*41 (2014) 065001. [arXiv:1401.4835](#), [doi:10.1088/0954-3899/41/6/065001](#).
- [16] T. S. Biro, A. Jakovac, Power-law tails from multiplicative noise, *Phys. Rev. Lett.* 94 (2005) 132302. [arXiv:hep-ph/0405202](#), [doi:10.1103/PhysRevLett.94.132302](#).
- [17] A. Khuntia, S. Tripathy, R. Sahoo, J. Cleymans, Multiplicity Dependence of Non-extensive Parameters for Strange and Multi-Strange Particles in Proton-Proton Collisions at $\sqrt{s} = 7$ TeV at the LHC, *Eur. Phys. J. A*53 (5) (2017) 103. [arXiv:1702.06885](#), [doi:10.1140/epja/i2017-12291-8](#).
- [18] H. Zheng, L. Zhu, A. Bonasera, Systematic analysis of hadron spectra in p+p collisions using Tsallis distributions, *Phys. Rev. D*92 (7) (2015) 074009. [arXiv:1506.03156](#), [doi:10.1103/PhysRevD.92.074009](#).
- [19] B. De, Non-extensive statistics and understanding particle production and kinetic freeze-out process from p_T -spectra at 2.76 TeV, *Eur. Phys. J. A*50 (2014) 138. [arXiv:1409.3079](#), [doi:10.1140/epja/i2014-14138-2](#).
- [20] R. N. Patra, B. Mohanty, T. K. Nayak, Centrality, transverse momentum and collision energy dependence of kinetic freeze-out parameters in relativistic heavy-ion collisions using Tsallis statistics [arXiv:2008.02559](#).
- [21] J. Cleymans, D. Worku, The Tsallis Distribution in Proton-Proton Collisions at $\sqrt{s} = 0.9$ TeV at the LHC, *J. Phys. G*39 (2012) 025006. [arXiv:1110.5526](#), [doi:10.1088/0954-3899/39/2/025006](#).
- [22] J. Cleymans, D. Worku, Relativistic Thermodynamics: Transverse Momentum Distributions in High-Energy Physics, *Eur. Phys. J. A*48 (2012) 160. [arXiv:1203.4343](#), [doi:10.1140/epja/i2012-12160-0](#).
- [23] J. Cleymans, M. Azmi, Large transverse momenta and Tsallis thermodynamics, in: *Journal of Physics: Conference Series*, Vol. 668, IOP Publishing, 2016, p. 012050.
- [24] T. Bhattacharyya, J. Cleymans, L. Marques, S. Mogliacci, M. Paradza, On the precise determination of the Tsallis parameters in proton-proton

- collisions at LHC energies, *Journal of Physics G: Nuclear and Particle Physics* 45 (5) (2018) 055001.
- [25] K. Aamodt, et al., Production of pions, kaons and protons in pp collisions at $\sqrt{s} = 900$ GeV with ALICE at the LHC, *Eur. Phys. J. C* 71 (2011) 1655. [arXiv:1101.4110](#), [doi:10.1140/epjc/s10052-011-1655-9](#).
- [26] B. B. Abelev, et al., Production of charged pions, kaons and protons at large transverse momenta in pp and Pb–Pb collisions at $\sqrt{s_{NN}} = 2.76$ TeV, *Phys. Lett. B* 736 (2014) 196–207. [arXiv:1401.1250](#), [doi:10.1016/j.physletb.2014.07.011](#).
- [27] J. Adam, et al., Multiplicity dependence of charged pion, kaon, and (anti)proton production at large transverse momentum in p-Pb collisions at $\sqrt{s_{NN}} = 5.02$ TeV, *Phys. Lett. B* 760 (2016) 720–735. [arXiv:1601.03658](#), [doi:10.1016/j.physletb.2016.07.050](#).
- [28] J. Adam, et al., Measurement of pion, kaon and proton production in proton–proton collisions at $\sqrt{s} = 7$ TeV, *Eur. Phys. J. C* 75 (5) (2015) 226. [arXiv:1504.00024](#), [doi:10.1140/epjc/s10052-015-3422-9](#).
- [29] S. Chatrchyan, et al., Study of the inclusive production of charged pions, kaons, and protons in pp collisions at $\sqrt{s} = 0.9, 2.76, \text{ and } 7$ TeV, *Eur. Phys. J. C* 72 (2012) 2164. [arXiv:1207.4724](#), [doi:10.1140/epjc/s10052-012-2164-1](#).
- [30] A. M. Sirunyan, et al., Measurement of charged pion, kaon, and proton production in proton-proton collisions at $\sqrt{s} = 13$ TeV, *Phys. Rev. D* 96 (11) (2017) 112003. [arXiv:1706.10194](#), [doi:10.1103/PhysRevD.96.112003](#).